

Clustering methods and Bayesian inference for the analysis of the evolution of immune disorders

A. Carpio ^{*}, A. Simón [†], L.F. Villa [‡]

September 25, 2020

Abstract. Choosing appropriate hyperparameters for unsupervised clustering algorithms could be an optimal way for the study of long-standing challenges with data, which we tackle while adapting clustering algorithms for immune disorder diagnoses. We compare the potential ability of unsupervised clustering algorithms to detect disease flares and remission periods through analysis of laboratory data from systemic lupus erythematosus (SLE) patients records with different hyperparameter choices. To determine which clustering strategy is the best one we resort to a Bayesian analysis based on the Plackett-Luce model applied to rankings. This analysis quantifies the uncertainty in the choice of clustering methods for a given problem.

1 Introduction

Since the early times of the introduction of mathematical methods for medical diagnosis [7], remarkable advances have been made. Nowadays, the increasing availability of medical data related to all sorts of illnesses is fostering the development of machine learning techniques [2] for medical diagnosis and treatment. While neural networks are often used for image based diagnosis [25, 16], supervised and unsupervised clustering techniques [22] are now widely employed to investigate the role of genes in sickness [17, 24, 4, 20] and to study the response to therapies [15, 6], as well as for assisted clinical diagnosis using information from digital devices [18, 21]. Developing tools to assess the reliability of such automatic procedures and to choose the best method for different situations and clinical environments has become essential [18].

We consider here the applicability of unsupervised clustering techniques to identify stages in time-dependent series of clinical data. More precisely, we focus on the study of immune disorders, such as SLE, difficult to diagnose and treat properly because many symptoms are non specific and change throughout the evolution of the disease. SLE is a chronic autoimmune disease in which

^{*}Universidad Complutense de Madrid, Spain

[†]Universidad Complutense de Madrid and Universidad de Granada, Spain

[‡]Hospital Universitario Puerta de Hierro de Madrid, Spain

the immune system attacks healthy tissues by mistake [1]. This attack causes inflammation and, in some cases, permanent tissue damage. Parts of the body commonly affected include skin, joints, heart, lungs, kidneys, red bone marrow (blood cell formation) and brain. Symptoms of lupus vary between people and may be mild to severe, affect one area of the body or many, come and go, and change over time. They include painful and swollen joints, fever, fatigue, chest pain when breathing deeply, hair loss, mouth ulcers, swollen glands, a red rash (typically on the face) and cardiac, renal or neural symptoms.

The cause of SLE is unknown. It is thought to involve genetics as well as environmental factors. Female sex hormones, race, age between 15 and 45 and family history appear to be risk factors for SLE development. Aside, emotional or physical stress, sunlight exposure, viral infections, certain drugs, pregnancy, giving birth, smoking or vitamin D deficiency can trigger disease flares. There is currently no cure for lupus. Treatments include nonsteroidal anti-inflammatory drugs, corticosteroids, immunosuppressants, hydroxychloroquine, and immunomodulatory monoclonal antibodies. However, dealing with a chronic disease makes one concerned about long-term adverse effects. Several treatments for lupus have attracted great attention recently due to their applicability to covid-19 patients. In fact, serious covid-19 cases develop similar hyperimmune responses [9] which damage the patient's tissues and may cause death.

Lupus patients go through periods of illness, called flares, and periods of wellness, called remission. The symptoms during flares vary. It is essential to be able to distinguish early when the patient is transitioning from remission to flares, as well as what factors are causing it. A great deal of information is contained in laboratory tests. Our purpose is to develop mathematical methods to process it automatically from time series of such tests. We show here that it could be possible to automatically detect transition days by applying clustering techniques. Different clustering strategies may produce variable results on the same datasets. Therefore, it is important to be able to assess which algorithms perform better in given tests problems. We show that a Bayesian analysis of rankings of the performance of clustering algorithms on medical datasets provides information on the probability of each clustering algorithm being the best.

The rest of the paper is organized as follows. Section 2 describes the datasets under study. Sections 3, 4 and 5 apply K-means, Hierarchical clustering and Density based spatial clustering to the selected datasets. Section 6 explains how to construct performance rankings to estimate the probability of a particular clustering procedure and hyperparameter choice to be the most adequate one to identify automatically transition from remission to flares and other stages in the patient evolution from time series of clinical data. We summarize our conclusions in Section 7. A final Appendix details the clinical variables under consideration.

2 Clustering clinical data

Laboratory tests are often used to diagnose lupus, since the illness involves an immune response by antibodies against the patients's own body. In addition, laboratory tests play a key role when detecting the transition to flares and identifying the kind of health disorder that is building up and needs to be treated. Tables 5-7 in the Appendix list some variables usually monitored. We will work here with 28 patient records, choosing one dataset to illustrate the outcome of the clustering procedures and all datasets for the Bayesian study of the probability of a specific method being the best to identify illness stages in these patient's records.

All datasets are normalized subtracting the mean from each variable and dividing by three times the variance. After that, we obtain normalized time series of clinical data as represented in Figure 1. A difficulty in dealing with time series of clinical data is that some measurements are usually missing. White boxes mark missing data. We will eliminate from our study all variables with more than 50% measurements missing. For the remaining variables, we fill empty boxes with the average value of the variable over the remaining days. Variables labeled as 17, 18, 28, 29, 30, 47, 48 in Tables 5-7 are suppressed. At the end, our data set is formed by 29 columns (days) and 65 rows (variables). From this set, we may also eliminate six more variables with essentially zero values. Time measurements are not consecutive (they are not recorded in consecutive days) but expand over months. The label attached to the days only indicates time ordering. Visually, we can identify three groups of days. Group 1 is formed by days 1 to 16, group 2 is formed by days 17 to 22, and group 3 is formed by days 23 to 29. The complementary representation in Figure 2 shows how certain variables get out of control as time advances, and later start coming back to normal, responding to treatment. These observations provide the motivation to look for clusters in clinical data.

Automatic clustering techniques may produce clusters even when the original data contain no significative clusters. Hopkins criterion [11] allows us to establish whether the dataset contains relevant clusters. Given a set D , the Hopkins statistics is obtained as follows:

1. We extract a uniform sample (p_1, \dots, p_n) from D formed by n points.
2. For each point $p_i \in D$, we find the closest neighbor p_j and denote the distance $x_i = \text{dist}(p_i, p_j)$.
3. We generate a random sample (q_1, \dots, q_n) with n points, which we call D_{random} from a uniform distribution keeping the same variance as the original set D .
4. For each $q_i \in D_{\text{random}}$, we find its closest neighbor q_j in D and denote $y_i = \text{dist}(q_i, q_j)$.

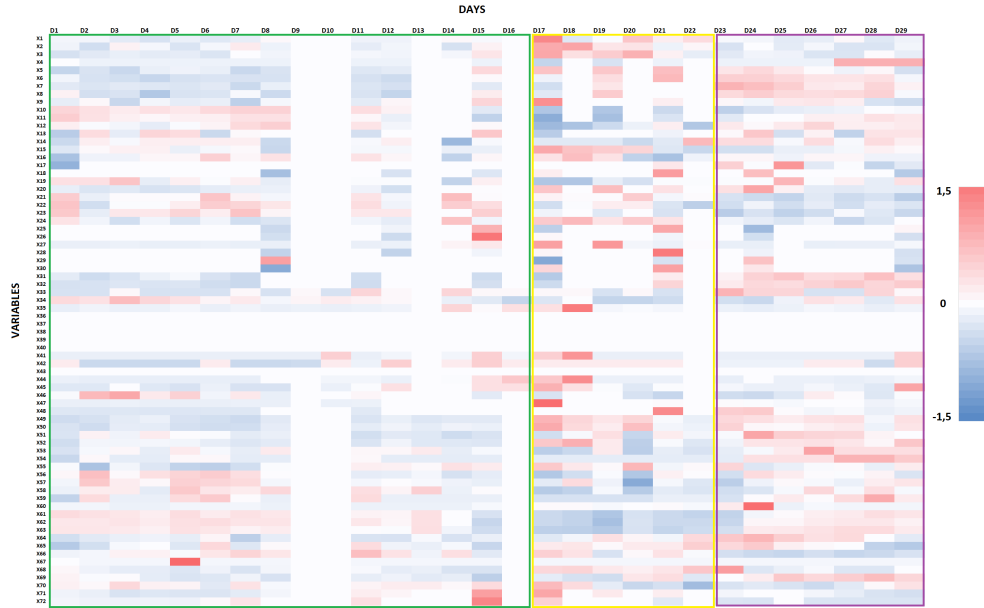


Figure 1: Heatmap of the reference time series of clinical data.

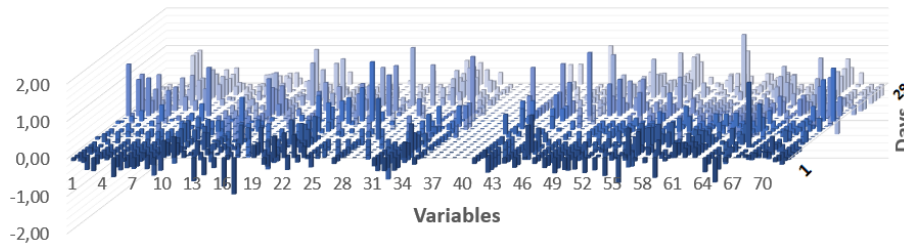


Figure 2: Bar histogram of the reference clinical data.

5. We calculate the Hopkins statistics as

$$H = \frac{\sum_{i=1}^n y_i}{\sum_{i=1}^n x_i + \sum_{i=1}^n y_i}.$$

If D was uniformly distributed, then the sums $\sum_{i=1}^n y_i$ and $\sum_{i=1}^n x_i$ would be similar, and H would be close to 0.5. However, if there are clusters present in D , the distances to the artificial points ($\sum_{i=1}^n y_i$) would be larger than those to the true points ($\sum_{i=1}^n x_i$) and H would be larger than 0.5. The larger is H , the more likely the presence of clusters in the data is.

For our dataset, $H = 0.655$, so that it makes sense applying clustering techniques. An additional issue when dealing with medical data, is whether such clusters have a medical meaning, which will be the case here.

3 K-means clustering

K-Means [14] is one of the most widely used unsupervised clustering algorithms. The idea is to group observations in clusters so that the total intra-cluster variation is minimized.

3.1 Algorithm description

Given an observation $\mathbf{x}_i = (x_{i,1}, \dots, x_{i,M})$ in a M dimensional space, a cluster C_j of points in the same space and the cluster centroid $\boldsymbol{\mu}_j$, we define the intra-cluster total variation as:

$$\sum_{j=1}^K W(C_j) = \sum_{j=1}^K \sum_{\mathbf{x}_i \in C_j} d(\mathbf{x}_i, \boldsymbol{\mu}_j),$$

where d represents the euclidean distance

$$d(\mathbf{x}_i, \boldsymbol{\mu}_j) = \sqrt{\sum_{\ell=1}^M (x_{i,\ell} - \mu_{j,\ell})^2}.$$

The centroids of each cluster C_j with $|C_j|$ observations are defined as the averages of the observations in the cluster, that is, $\boldsymbol{\mu}_j = \sum_{\mathbf{x}_i \in C_j} \mathbf{x}_i / |C_j|$. The intra-cluster total variation can be interpreted as a measure of the cluster compactness. Each term $W(C_j)$ is the intra-cluster variation for a single cluster:

$$W(C_j) = \sum_{\mathbf{x}_i \in C_j} d(\mathbf{x}_i, \boldsymbol{\mu}_j),$$

where \mathbf{x}_i are the points belonging to the cluster C_j . In our case, each observation is formed by measurements of M clinical variables a specific day.

Once the number k of clusters to be formed is specified, the K-Means algorithm proceeds in the following steps:

1. We initialize the centroids $\boldsymbol{\mu}_j$ generating generate k random points in the M dimensional space.
2. Each observation \mathbf{x}_i is assigned to the closest centroid according to the euclidean distance.
3. For each cluster, we update the centroid as the average of the cluster observations.
4. We minimize the total intra-cluster variation iteratively. To do so, we iterate the previous steps until the clusters do not change or the maximum number of iterations is surpassed.

The main drawback of this algorithm is the need of knowing the number of clusters beforehand. We describe some strategies to estimate it next.

3.2 Selection of the number of clusters

Two methods can be used to estimate the number of clusters in K-Means: the Elbow method and the Silhouette method. While the Elbow method favors cluster compactness, the Silhouette analysis opts for cluster separation when selecting k .

The Elbow method is based on running K-Means for different choices of the number of clusters. Each run stores the total intra-cluster variation. The number of clusters N is selected in such a way that the total intra-cluster variation does not diminishes noticeably for $k + 1$. This can visualized graphically, plotting the total intra-cluster variation as a function of k . When applied to our reference clinical dataset, we find Figure 3(a), which suggests $k = 3, 4, 5$ as reasonable values.

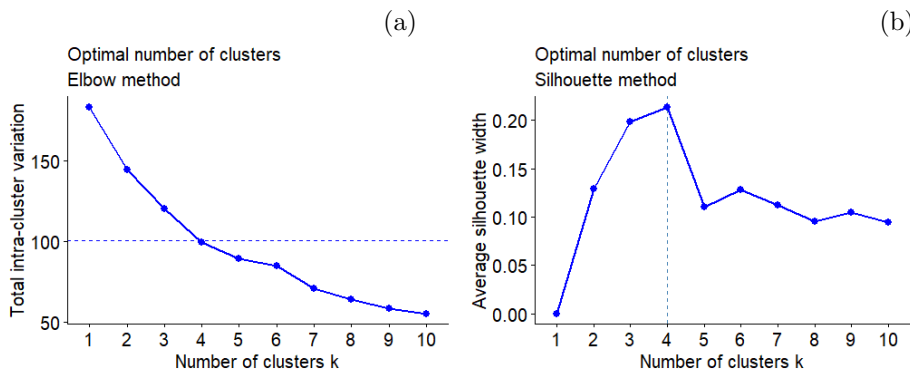


Figure 3: (a) Elbow Method: Change in the total intra-cluster variation as a function of the number of clusters k . (b) Silhouette method: Silhouette coefficient as a function of the number of clusters k .

The Silhouette analysis [13] measures cluster quality. This method determines the quality of a cluster estimating how well the point fits in the cluster. This is done calculating the mean distance from each point to the other clusters, the so-called Silhouette coefficient. Choosing the number of clusters maximizing the Silhouette coefficient we guarantee a sharp separation between clusters. Figure 3(b) represents the Silhouette coefficient as a function of k for our reference dataset. The value maximizing the coefficient is $k = 4$, though $k = 3$ is only slightly worse.

3.3 K-Means applied to a time series of clinical data

The results obtained running K-Means for $k = 3$ and $k = 4$ clusters are represented in Figures 4 and 5.

As Figure 4 shows, the algorithm is able to identify groups of days, which are almost consecutive. The first (red) group includes days 21 to 29. The second (green) group includes days 1 to 16, skipping day 15. Finally, the third (blue)

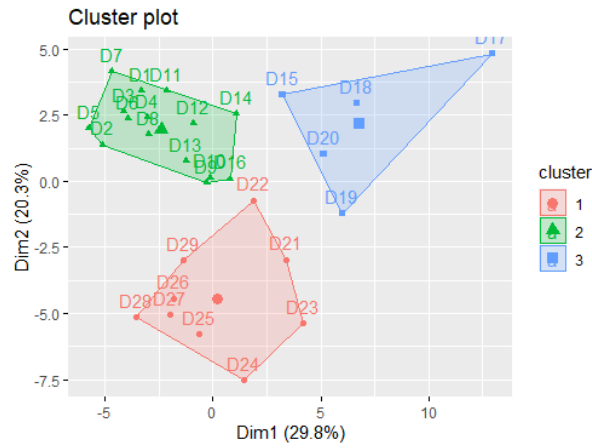


Figure 4: Clusters obtained with K-Means when $k = 3$.

group includes days 17 to 20, and also day 15. Notice that day 15 is an anomaly for K-Means.

Let us see the behavior for $k = 4$. Again, Figure 5 shows, that the algorithm is able to identify groups of days. The first (red) group includes days 1 to 13. The second (green) group includes days 17 and 18. The third (blue) group includes days 24 to 29. Finally, the fourth (magenta) group includes days 14 to 16, plus days 19-23. This time days 17-18 are an anomaly for K-Means.

As a conclusion, days 15, 17 and 18 are difficult to explain for this algorithm. This may mean that they are days at which the patients' condition changes.

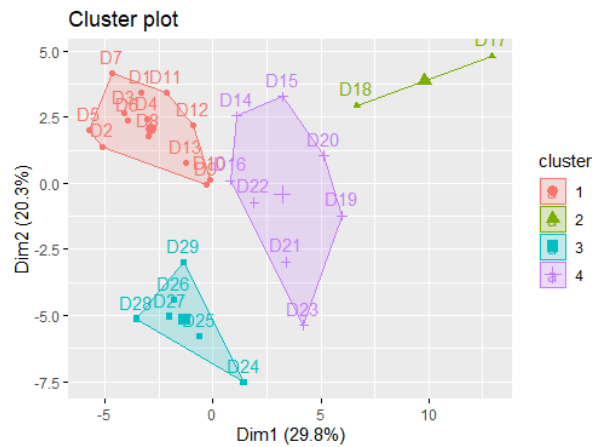


Figure 5: Clusters obtained with K-Means when $k = 4$.

4 Hierarchical clustering

Hierarchical clustering [23] is a popular strategy for unsupervised learning. We will use here the agglomerative version of the algorithm, which works bottom up. Each element is initially considered a cluster itself. A cluster formed by a single element is a leaf. At each step, the two most similar clusters merge to form a bigger one, called node. This process is repeated progressively until all the points are combined in a big cluster, the tree.

4.1 Algorithm description

This algorithm requires a similarity measure between elements and a strategy to merge clusters. Different distances can be selected as similarity measures. Here we use the euclidean distance. The elements to be compared are the values of the M variables for different days. Considering them points in a M dimensional space, we can compute the euclidean distance between them. Regarding the clustering strategy, we calculate the distances between all the elements and use the 'complete' approach. Each node's height in the tree represents the distance between the two subnodes merged at that node. All leaves below any node whose height is less than a threshold C are grouped into a cluster (a singleton if the node itself is a leaf). This process is represented in a dendrogram, a graph representing how the clusters merge until they form the tree that contains them all. As we move upwards the most similar clusters combine in branches that merge later at a higher height, known as the cophenetic distance between the clusters. The higher that height, the more different the clusters are.

Once a hierarchical tree is built, we have to check whether it is representative of our set of data, that is, whether the heights represent the original distances with reasonable accuracy. To do so, we calculate the correlation between the cophenetic distance and the original distance used to check similarity between objects, the euclidean distance in our case. If the correlation coefficients displays a large coefficient in a linear relation, say, larger than 0.75, the tree is considered a good representation of the dataset. Selecting a particular height to cut the tree, we obtain different numbers of clusters.

4.2 Hierarchical clustering applied to a time series of clinical data

In this section we use the hierarchical clustering to select the onset of severe illness periods in time series of measurement of the clinical variables of lupus patients. The dendrograms in Figure 6 and 7 show the outcome of applying agglomerative hierarchical clustering based on the euclidean distance cut at a different height. The resulting tree is a good representant of the data set, since the correlation between the cophenetic distance and the euclidean distance is $0.7767 > 0.75$. We select the hyperparameter, that is, the height, in such a way that we obtain the number of clusters we considered with K-means. In the first case, choosing a threshold height to have 3 clusters, days 15, 17, 18 are singled

out. In the second one, with 4 clusters, day 17 is marked as possible onset. Days 15, 17, 18 are automatically identified as days at which the patients condition may change significantly again.

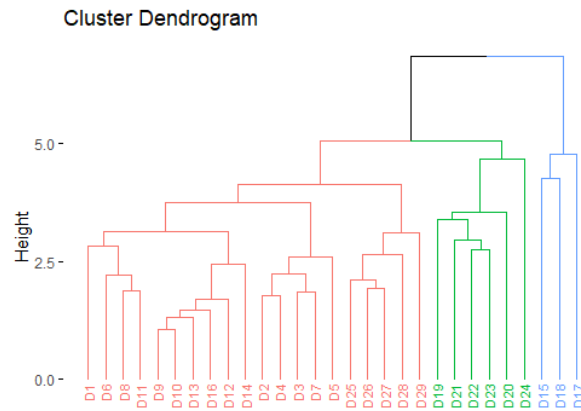


Figure 6: Dendrogram representing 3 clusters in the time sequence of clinical variables

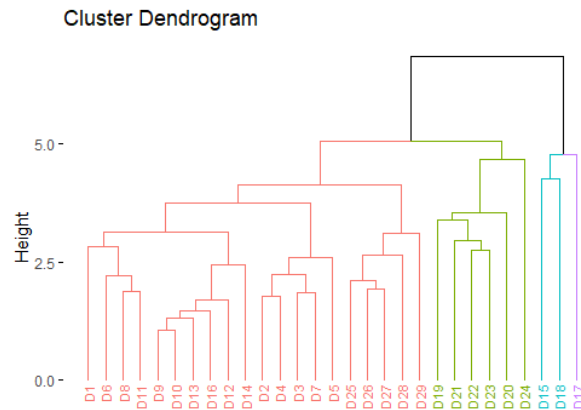


Figure 7: Dendrogram representing 4 clusters in the time sequence of clinical variables

4.3 Grouping clinical variables

Both K-Means and hierarchical clustering select the same days to mark a strong alteration in the status of a patient. We can analyze the clinical variables by a

combination of both.

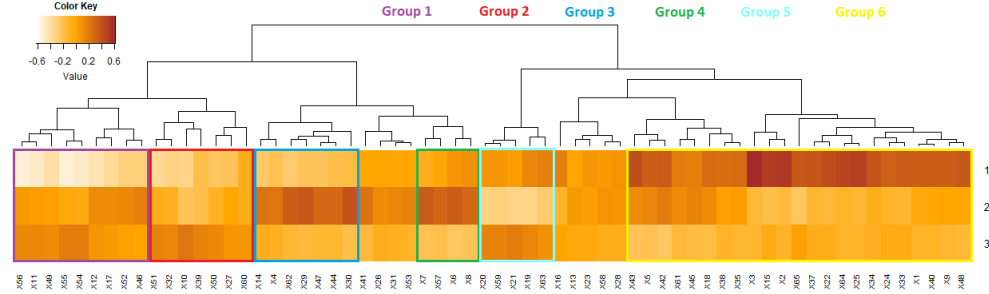


Figure 8: Heatmap of the matrix relating the K-Means centroids for the $k = 3$ clusters of days and the clinical variables. We have superimposed a dendrogram classifying the variables in groups according to their influence in the cluster centroids.

K-Means algorithm provides a matrix describing how each variable influences the final centroids. We represent this matrix by means of a heatmap for $k = 3$ clusters, see Figure 8. Then, we superimpose a dendrogram grouping the variables by similarity. In this way, we distinguish 6 groups of variables according to their interactions through the clusters. Considering high values the largest positive ones, intermediate values those about 0 and small values the largest negative ones, we observe:

- The low values of group 1 identify the first cluster, while intermediate values are typical of the second and third clusters.
- The low values of group 2 identify the first cluster, while intermediate values are typical of the second cluster and large values of the third cluster.
- The large values of group 3 identify the second cluster, while small values are typical of the first and second clusters.
- The large values of group 4 identify the second cluster, while small values are typical of the third cluster and intermediate values of the first cluster.
- The low values of group 5 identify the second cluster, while intermediate-large values are typical of the first and third clusters.
- The large values of group 6 identify the first cluster, while intermediate-small values are typical of the second and third clusters.

A few variables remain almost constant through the clusters and we have left them unassigned. This shows that they have little effect on the overall clustering results and we may as well suppress them. These relations are illustrated in Table 4.3. Variables for which the heat map reports large positive values within the cluster affect strongly the centroid: its coordinate in the direction of that

variable is large. Considering variables for which the heat map reports small values (that is, large negative values) within the cluster, the centroid varies strongly in the opposite direction. In practice, this information would allow to track automatically which variables play relevant roles in each cluster of days and motivate the change.

	Large	Intermediate	Low
Group 1	2-3	2-3	1
Group 2	3	2	1
Group 3	2	1-3	1-3
Group 4	2	1	3
Group 5	1-3	1-3	2
Group 6	1	2-3	2-3

Table 1: Relation between day clusters and clinical variable blocks.

5 Density-based spatial clustering

The Density-Based Spatial Clustering of Applications with Noise (DBSCAN) algorithm usually allows us to detect clusters of any structure even in the presence of noise and outliers. This technique is based on the spatial density of points, following human intuition to identify clusters. For instance, in Figure 9, we visually spot four clusters in spite of the presence of noise due to the point density variations.

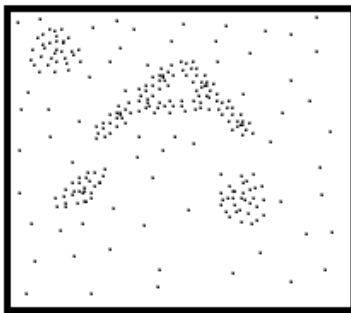


Figure 9: Density based cluster identification in the presence of noise.

The method looks for high density regions and assigns clusters to them, while points in less dense regions are left outside and become anomalies. This is the main advantage of this algorithm: being able to detect outliers. Another advantage is that methods such as K-Means and Hierarchical Clustering are designed to find spherical or convex clusters, that is, they work well when we must find well separated and compact clusters, which is not always the case.

Moreover, K-Means also needs to classify all the points in one cluster forcing the introduction of weird criteria to detect outliers.

5.1 Algorithm description

The DBSCAN algorithm is governed by two hyperparameters:

- ϵ : Smallest distance for two points to be considered neighbors.
- *MinPts*: Minimum number of points required to form a cluster.

According to them, we distinguish three types of points:

- Core Point: Any point with a number of neighbors greater than or equal to a fixed minimum value *MinPts* (including itself).
- Border Point: Any neighbor of a core point with a number of neighbors smaller than *MinPts*.
- Outlier: Any point which is not a core neither a border point.

Figure 10 illustrates the three types of points for a given ϵ and *MinPts* = 6. Point **x** is a core point, it has at least 5 neighbors at a distance smaller than ϵ , a total of 6 points counting **x**. On the other hand, **y** is a border point, since the number of neighbors is smaller than 6, but it is a neighbor of the core point **x**. Finally, **z** is an outlier. Although it is a neighbor of **y**, it is not a neighbor of any core point and it has less than 6 neighbors.

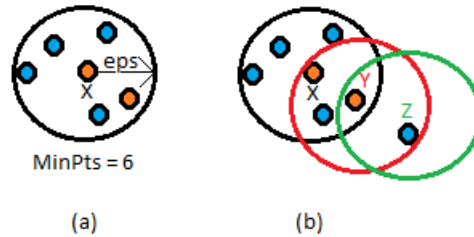


Figure 10: Cluster detection in the presence of noise by density criteria.

Before describing the algorithm in detail, we need to distinguish three concepts:

- Directly reachable points: A point *A* is directly reachable from *B* when it is a neighbor of *B* and *B* is a core point.
- Reachable points: A point *A* is reachable from *B* when we can find a set of core points from *B* to *A*.

- **Connected point:** Two points A and B are connected when there is a core point C such that A and B are reachable from C .

A density based cluster is a group of connected points. The DBSCAN algorithm works as follows:

1. For each point \mathbf{x}_i , we calculate the distance between \mathbf{x}_i and the remaining points. Then, we find all the neighbors within the radius ε and mark as core points those with a number of neighbors greater or equal to $MinPts$.
2. For each core point not yet assigned to a cluster, we create a new cluster. Next, we search for all the points connected to that core point and assign them to that cluster.
3. We repeat those steps over the remaining set of points.
4. The points not assigned to any cluster after this process are considered outliers.

5.2 Hyperparameter tuning

Determining adequate values for ε and $MinPts$ is a difficult task, strongly conditioned by the structure of the dataset we are working with. In general, there is no automatic procedure to do so. The main problems caused by a poor choice are:

- If the value of ε is too small, there will not be enough points to form clusters and most points risk being classified as outliers. On the other hand, if ε is too large, most points will be classified in clusters and we will not be able to identify the outliers.
- If $MinPts$ is too large, too many points are required to form a cluster. Dense regions may be classified as outliers. When it is too small, low density regions would appear as clusters and outliers would remain undetected.

These values have to be carefully tuned to detect meaningful outliers. Our choice will be to find optimal values of ε given $MinPts$. We start calculating the means of the distances to the k closest points and represent them in increasing order. Turning points will mark thresholds for sharp changes and will provide candidate values for ε .

5.3 DBSCAN applied to a time series of clinical data

In this section we explain how to use the clustering algorithm DBSCAN [8] to select the onset of severe illness periods in time series of measurement of the clinical variables of lupus patients.

We select ε fixing the hyperparameter $MinPts = 3$, minimum number of days in clusters usually observed in our previous studies. The resulting graph

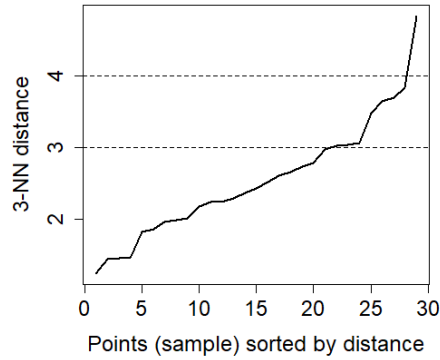


Figure 11: Graph of ascending 3-distances for the reference dataset of medical variables.

would be We appreciate two turning points, at $\varepsilon = 3$ and $\varepsilon = 4$. However, $\varepsilon = 4$ is too large and all the points form a cluster. Running the algorithm with $\varepsilon = 3$ and $\varepsilon = 3.5$ we find the following.

For $MinPts = 3$ and $\varepsilon = 3$, there are five outliers. The first one (day 15) marks the correct onset of the sickness period, see Figure 12(a). On the other hand, when $MinPts = 3$ and $\varepsilon = 3.5$, we find a single outlier (day 17), two days later, see Figure 12(b). This technique confirms what we have previously observed: the clinical variables are strongly altered between the days 15 and 17.

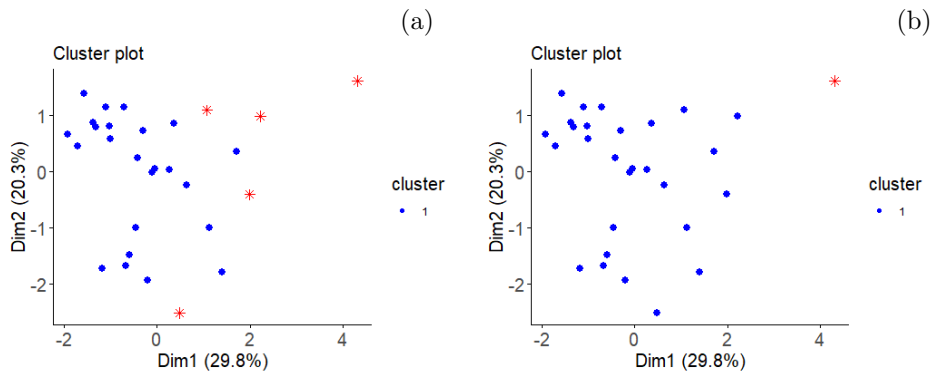


Figure 12: (a) Clusters and outliers with DBSCAN and $\varepsilon = 3$. (b) Clusters and outliers with DBSCAN and $\varepsilon = 3.5$.

6 Bayesian inference for clustering performance

For the same set of data, results vary using different clustering procedures. Thus, comparing the performance of different clustering strategies to extract useful information from clinical datasets is an important task. In the previous sections, we have illustrated the use of clustering strategies on a dataset to obtain information on the phases of the illness of a patient, in particular, to characterize the onset of deterioration and recovery periods. Next, we describe how to infer in an automatic way which methods are more adequate for particular collections of clinical records by combining the construction of rankings on smaller collections of selected datasets and Bayesian analysis.

6.1 Bayesian inference for ranking analysis

The idea is to run the clustering methods to be compared on a number of datasets for which the diagnosis is known, and then rank them according to their performance. Finally, we analyze the results using a Plakett-Luce (PL) Bayesian model [5, 12]. This model is well adapted to this type of problems and differs from other approaches for continuous problems [3].

An advantage of PL models is that normalized parameters represent directly the marginal probability of an algorithm being placed in first position. Another advantage is that it relies on a finite number of parameters, as many as algorithms we compare. It also fulfill's Luce's axiom: 'The probability of an algorithm A of being placed before algorithm B is the same independently of the remaining algorithms'.

The PL model combines three ingredients:

1. It selects randomly the algorithm to be positioned.
2. Each algorithm has a weight w_i , and the probability to select an algorithm at each stage is the ratio between its weight and the sum of the weights of the remaining algorithms.
3. Representing by $\sigma = (\sigma_1, \dots, \sigma_n)$ a ranking of size n , where $\sigma_i = j$ implies that the j -th algorithm is located at the i -th position and by $w = (w_1, \dots, w_n)$ the vector of weights, the PL probability to select that ranking is:

$$P_{PL}(\sigma) = \prod_{i=1}^n \frac{w_{\sigma_i}}{\sum_{j=i}^n w_{\sigma_j}}.$$

By simplicity, we assume that the sum of weights is 1.

More precisely, the process, schematized in Figure 13, is the following:

1. Run the clustering algorithms over m datasets. Choosing a way to evaluate the performance of the algorithms, we will have a matrix \mathbf{M} in which $M(i, j)$ is the performance of algorithm j on dataset i .

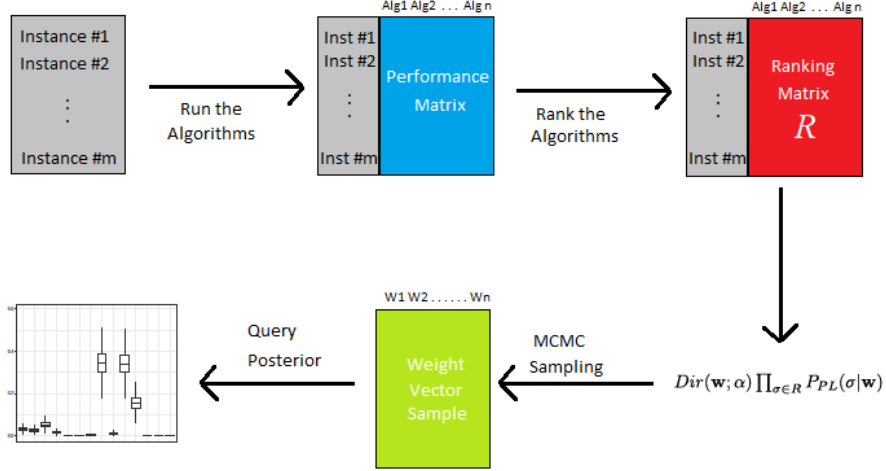


Figure 13: Scheme for the Bayesian analysis of clustering ranking performance.

2. Assign a position in the ranking to each algorithm: the greatest the performance, the higher the situation in the ranking. In this way, we obtain a matrix \mathbf{R} , where $\mathbf{R}(i, j)$ is the location in the ranking of algorithm j applied to dataset i .
3. A given matrix \mathbf{R} gives partial information of the likelihood of different clustering algorithms to perform better than the rest. We quantify the uncertainty in such conclusions using Bayes relation for conditional probabilities

$$P(\mathbf{w}|\mathbf{R}) \propto P(\mathbf{w}) \cdot P(\mathbf{R}|\mathbf{w}),$$

where $\mathbf{w} = (w_1, \dots, w_n)$ denote the PL parameters. Since we are assuming $\sum_{i=1}^n w_i = 1$, they represent the probability of having a given algorithm in the first position. We set

$$P(\mathbf{R}|\mathbf{w}) = \prod_{\sigma \in \mathbf{R}} P_{PL}(\sigma, \mathbf{w}),$$

$$P(\mathbf{w}) = \text{Dir}(\mathbf{w}, \boldsymbol{\alpha}),$$

where the Dirichlet distribution models uncertainty in the weights.

4. Since the posterior distribution does not have a closed form, we sample it using Markov Chain Monte Carlo (MCMC) methods [10]. From the set of samples, we visualize uncertainty in the probability of a clustering strategy being the best by means of histograms or expected values.

The Dirichlet distribution $\text{Dir}(\boldsymbol{\alpha})$ is a family of multivariate distributions parametrized by a vector $\boldsymbol{\alpha}$ of real positive numbers. It generalizes the Beta

function. The Dirichlet distribution of order $K \geq 2$ with positive parameters $\alpha_1, \dots, \alpha_K$ has a density function

$$f(x_1, \dots, x_K; \alpha_1, \dots, \alpha_K) = \frac{1}{B(\boldsymbol{\alpha})} \prod_{i=1}^K x_i^{\alpha_i-1}$$

where $\sum_{i=1}^K x_i = 1$ and $x_i \geq 0$ for $i \in [1, K]$. The normalization constant is a multivariate Beta function expressed in terms of Gamma functions as:

$$B(\boldsymbol{\alpha}) = \frac{\prod_{i=1}^K \Gamma(\alpha_i)}{\Gamma(\sum_{i=1}^K \alpha_i)} \quad \boldsymbol{\alpha} = (\alpha_1, \dots, \alpha_K).$$

Since we lack information on the performance of the algorithms for general datasets, we use a uniform distribution for the hyperparameter $\boldsymbol{\alpha}$, that is, $\alpha_i = \alpha = 1, i = 1, \dots, n$.

6.2 Plackett Luce method applied to time series of clinical data

We apply our clustering techniques to identify groups of days reflecting different stages of the evolution of the patient. We consider the clinical records of 28 patients which have been previously diagnosed. In many cases there are sickness periods which require special medical care, starting a known specific day. This results in a time series of measurements of clinical variables, which display a different behavior before and after it. A way to quantify the performance of the different algorithms of the datasets is to check how well they predict the onset of that flares period. Therefore, we need to define an automatic criterion to identify it based on the different clustering strategies:

- For the DBSCAN algorithm we select the first day not assigned to any cluster, that is, the first outlier.
- For K-Means, we choose the first day which is unsequentially classified, that is, which has no neighbors in the same cluster. When such a day is not found, we choose the first day of the smallest cluster.
- For hierarchical clustering, we choose the smallest of the last isolated points to merge with existing clusters. If not found, we choose the first day within the smallest cluster.

Performance is quantified by means of the difference between the day estimated from the clustering analysis and the known true transition day.

Let us revise the clustering analysis performed on our test dataset and apply these criteria. The onset of an instability period for the patient is defined by Day 15.

- For DBSCAN with $MinPts = 3$ and $\varepsilon = 3$, we had five outliers in Figure 12(a). The smallest corresponds to day 15. The distance is $D = 0$. When $k = 3$ and $\varepsilon = 3.5$, we had one outlier in Figure 12(b), day 17. The distance is $D = 2$.
- K-Means with $k = 3$ introduces the first temporal mismatch on day 15, assigning this day to the third cluster (blue), instead of the second cluster (green), see Figure 12. The distance is $D = 0$. When $k = 4$, we have a mini-cluster with days 17 and 18. The distance is $D = 2$. When $k = 5$, the first temporal mismatch happens for day 11, and the distance is $D = 4$.
- Hierarchical clustering with 4 clusters, as depicted in Figure 7, singles out day 17. Therefore the distance is $D = 2$. Figure 6 considers 3 clusters instead. The smallest day in the smallest cluster is 15, thus the distance is $D = 0$.

We have applied these methods to 28 different clinical datasets, quantifying for each one the distance between the predicted and true transition days. We have excluded some datasets for several reasons. On three of them all the algorithms gave the same answer. Three more are discarded because the Hopkins statistics is too small to support looking for clusters. The variables just fluctuate. Three additional datasets are too complicate to analyze since they seem to present several periods of flares and remission, and should be divided in smaller periods. Thus, we study the remaining 19 datasets, which present only one transition. The results are represented in Table 2, where HC stands for hierarchical clustering (3C with 3 clusters, 4C with 4 clusters) and KM by K-Means.

Based on those distances, we build the ranking presented in Table 3. We assign a higher position in the ranking to smaller distances. The smallest possible distance is $D = 0$. Smallest distances rank first. Ties are solved assigning the same position to tied algorithms and freeing the next positions in equal number. Following this procedure, we obtain Table 3.

We notice that K-Means with $k = 3$, Hierarchical clustering with 3 clusters and DBSCAN with $\varepsilon = 3$ and $MinPts = 3$ perform quite well. We will use the PL method to determine the probability for each algorithm being the best, as well as the uncertainty in our choice of algorithm. Notice that there are repetitions in the ranking, obtaining the results represented in Table 6.2.

The results in Table 6.2 indicate that hierarchical clustering with 4 clusters is the algorithm performing best, with a probability of 21.30%. Next, it follows K-means with 3 clusters, with a 20.36% probability, which worsens increasing the number of clusters. DBSCAN appears with probability 18.73%.

In spite of the narrow differences, hierarchical clustering algorithms outperform the rest due to two reasons. First, they adapt well to small datasets. Second, they do not require a previous knowledge of the number of clusters, one can infer reasonable values from the tree. DBSCAN algorithms perform worse than expected. This algorithm is devised to look for outliers, since it does not need to place all points in a cluster, unlike K-means. However, for many

Distance to transition days	KM k=3	KM k=4	KM k=5	HC 3C	HC 4C	DBSCAN MinPts=3, $\epsilon=3$
D15	0	2	4	0	2	0
D4	0	1	1	0	0	0
D9	0	6	6	9	9	2
D3	2	2	2	0	0	0
D1	2	2	0	2	2	0
D1	6	10	10	0	0	0
D16	6	6	9	19	19	15
D14	0	0	11	0	0	0
D5	0	1	1	0	0	0
D9	0	5	5	3	5	5
D19	0	0	16	17	0	17
D50	41	41	41	4	0	0
D1	3	0	0	0	0	0
D23	22	22	41	0	0	21
D17	0	9	9	0	0	12
D19	14	14	14	0	7	18
D11	6	0	0	0	0	4
D3	21	14	0	19	21	0
D12	11	0	0	11	0	10

Table 2: Distances to the transition day for the different algorithms.

parameter choices we may find no outliers. Analyzing the results, we observe that either it gives sharp predictions or it produces the worst predictions. This may reflect a difficulty in tuning the hyperparameters in these algorithms, we just used the values selected for the reference case. On the other hand, K-Means is a classical algorithm that performs poorly in outlier detection. This is due to the need of placing all points in a cluster, the difficulty to handle non convex clusters, and the requirement of a priori information on the number of clusters.

Let us finally point out that the results vary with the definitions of transition days and distances for the different algorithms. If we adopt a different definition for hierarchical clustering techniques exploiting the cophenetic distances, then it outperforms the rest. Here we chose the simplest definitions to illustrate the procedure.

7 Conclusions

Extracting information from real clinical data in an automatic fashion faces a number of challenges, such as the unavailability of large enough amounts of data and incompleteness of the records, for instance. For each patient undergoing the same illness, slightly different variables may have been monitored and time intervals between tests vary largely. Unsupervised clustering methods provide

N	KM k=3	KM k=4	KM k=5	HC 3C	HC 4C	DBSCAN MinPts=3, $\epsilon=3$
1	1	4	6	1	4	1
2	1	5	5	1	1	1
3	1	3	3	5	5	2
5	4	4	4	1	1	1
6	3	3	1	3	3	1
7	4	5	5	1	1	1
8	1	1	3	5	5	4
9	1	1	6	1	1	1
10	1	5	5	1	1	1
11	1	3	3	2	3	3
12	1	1	4	5	1	5
14	4	4	4	3	1	1
15	6	1	1	1	1	1
18	4	4	6	1	1	3
23	1	4	4	1	1	6
24	3	3	3	1	2	6
27	6	1	1	1	1	5
28	5	3	1	4	5	1
29	5	1	1	5	1	4

Table 3: Rankings generated from the distances to the transition day in Table 2.

KM k=3	KM k=4	KM k=5	HC 3C	HC 4C	DBSCAN MinPts=3, $\epsilon=3$
0,148702	0,137208	0,11005	0,20365	0,213026	0,187354

Table 4: Results obtained applying the Plackett Luce method to the ranking in Table 3.

a tool to obtain basic information. We have compared the potential of DBSCAN, K-means and hierarchical clustering techniques to detect the presence of transitions from remission to flares in lupus patients using the time records of standard laboratory tests. When faced with large numbers of data sets, one must figure out which clustering strategy is likely to be the best one for most of them. We show that a Bayesian analysis based on the Plackett-Luce model applied to performance rankings of clustering algorithms on a collection of model clinical datasets may identify the best methods with quantified uncertainty.

Ideally, one would like to go further and identify patterns representing a type of flare in the data, to which new datasets could be compared. In that way, we might be able to diagnose automatically what particular manifestation of lupus we need to treat. This is a challenge due to the fact that available hospital records usually display different variable collections measured over irregular time

periods, reacting often to emergencies.

Acknowledgements. This research has been partially supported by the FEDER /Ministerio de Ciencia, Innovación y Universidades - Agencia Estatal de Investigación grant No. MTM2017-84446-C2-1-R. The authors thank Hospital Universitario Puerta de Hierro (Madrid, Spain) for providing the clinical data.

Appendix: Clinical variables.

We list here the clinical variables involved in the test datasets under study, see Tables 5 and 7. The labels refer to the variables involved in the reference dataset used through the text to exemplify the performance of clustering algorithms. The ranking for the Bayesian analysis uses additional datasets containing measurements of most of these variables. As it is to be expected from patients' records stored in hospitals, the datasets do not always record all the variables, and the days at which measurements are taken vary with the patient.

Blood Test - Variable	Label	Urine Test - Variable	Label
Glucose	1	pH	33
Urea	2	Density	34
Creatinine	3	Proteins (strip)	35
Glomerular Filtration	4	Glucose	36
Uric Acid	5	Ketone bodies	37
Cholesterol	6	Bilirubin	38
Cholesterol HDL	7	Urobilinogen	39
Cholesterol LDL	8	Nitrites	40
Triglyceride	9	Leukocytes	41
Total Proteins	10	Red blood cell	42
Albumin	11	Turbidity	43
Calcium	12	Sediment Comment	
Phosphorus	13	Leukocytes per field	44
Sodium	14	G6PD quantification	
Potassium	15	Red blood cell shadow	45
Chloride	16	Hyaline cylinders	
Bicarbonate	17	Cell Peeling	
Iron	18	Creatinine	46
Total Bilirubin	19	Proteins	
Creatine Kinase (CK)		Albumin	47
Lactate dehydrogenase (LDH)	20	Microalbumin/Creat. Ratio	48
Alanine Aminotransferase (ALT/GPT)	21	Haptoglobin	
Aspartate Aminotransf. (AST/GOT)	22		
Phosphatase Alkaline	23		
Gamma Glutamyltransferase (GGT)	24		
Vitamin B12	25		
Folic Acid	26		
C-Reactive Protein	27		
Ferritin	28		
Transferrin	29		
Transferrin Saturation	30		
Complement component 3 (C3)	31		
Complement component 4 (C4)	32		
Thyroid Stimulating Hormone (TSH)			
Parathyroid Hormone (PTHi)			
v25-OH Vitamin D			

Table 5: Numbering of clinical variables.

Hematology Laboratory - Variable	Label
Leukocytes	49
Neutrophils	50
Lymphocytes	51
Monocytes	52
Eosinophils	53
Basophils	54
Neutrophils (Percent)	55
Lymphocytes (Percent)	56
Monocytes (Percent)	57
Eosinophils (Percent)	58
Basophils (Percent)	59
Immature Granulocyte (IG) count	60
Red blood cell	61
Hemoglobin	62
Hematocrit	63
Mean Corpuscular Volume (MCV)	64
Mean Corpuscular Hemoglobin (MCH)	65
Mean Corpuscular Hemoglobin Concentration (MCHC)	66
Erythroblasts	
Erythroblasts (Percent)	67
Red blood cell Distribution Width (RDW)	68
Platelets	69
Platelet Distribution wWidth (PDW)	70
Reticulocytes (Percent)	
Erythrocyte Sedimentation Rate (ESR)	71
Direct Coombs	
Glucose-6-Phosphate Dehydrogenase (G6PD) quantification	
Haptoglobin	
Protrombrine Time	
Activated Partial Thromboplastin Time (APTT)	
Fibrinogen	
Lupus anticoagulant	
Immunology Laboratory - Variable	Label
Anti-dsDNA antibodies	72
IgM Anti-cardiolipin antibodies	
IgG Anti-cardiolipin antibodies	
IgM AntiB2glicoprotein-I antibodies	
IgG AntiB2glicoprotein-I antibodies	

Table 6: Numbering of clinical variables.

References

- [1] L. Arnaud, R. van Vollenhoven, Advanced Handbook of Systemic Lupus Erythematosus, ADIS, Springer International Publishing AG, 2018
- [2] Ch. Bishop, Pattern Recognition and Machine Learning, Springer-Verlag, 548-554, 2006
- [3] A. Carpio, S. Iakunin, G. Stadler, Bayesian approach to inverse scattering with topological priors, Inverse Problems 2020, DOI: 10.1088/1361-

- [4] A. Carpio, LL Bonilla, JC Mathews, A Tannenbaum, Fingerprints of cancer by persistent homology, bioRxiv 777169, 2019.
- [5] B. Calvo, J. Ceberio, J.A. Lozano, Bayesian inference for algorithm ranking analysis, in GECCO (2018), 'Genetic and Evolutionary Computation Conference Companion', Kyoto, Japan. ACM, New York, NY, USA, 2018
- [6] A. Carlier, A. Vasilevich, M. Marechal, J. de Boer, L. Geris, In silico clinical trials for pediatric orphan diseases, Scientific Reports 8, 2465, 2018.
- [7] J. Croft, R.E. Machol, Mathematical methods in medical diagnosis, Annals of Biomedical Engineering 2, 69-89, 1974.
- [8] M. Ester, H.P Kriegel, J. Sander, X. Xu, A density-based algorithm for discovering clusters in large spatial databases with noise, in Proceedings of the Second International Conference on Knowledge Discovery and Data Mining, AAAI Press, 226-231, Portland, Oregon 1996
- [9] F. Ferro, E. Elefante, C. Baldini, E. Bartoloni, I. Puxeddu, R. Talarico, M. Mosca, S. Bombardieri, COVID-19: the new challenge for rheumatologists, Clinical and Experimental Rheumatology, 175-180, 2020
- [10] W.R. Gilks, S. Richardson, D. Spiegelhalter, Markov chain Monte Carlo in practice, CRC press, 1995
- [11] B. Hopkins, J.G. Skellam, A new method for determining the type of distribution of plant individuals, Annals of Botany 18(2), 213-227, 1954.
- [12] E. Irurozki, B. Calvo, J.A. Lozano, PerMallows: An R Package for Mallows and Generalized Mallows Models, Journal of Statistical Software 71(12), 2016.
- [13] L. Kaufman, P.J. Rousseeuw, Finding groups in data : An introduction to cluster analysis, Hoboken, NJ: Wiley-Interscience, 1990.
- [14] J. MacQueen, Some methods for classification and analysis of multivariate observations, in Proceedings of the Fifth Berkeley Symposium on Mathematical Statistics and Probability, Volume 1: Statistics, 281-297, University of California Press, Berkeley, Calif., 1967.
- [15] M. Pouryahya, J.H. Oh, J.C. Mathews, J.O. Deasy, A.R. Tannenbaum, Characterizing cancer drug response and biological correlates: A geometric network approach, Scientific Reports 8, 6402, 2018.
- [16] P. Rajpurkar, J. Irvin, K. Zhu, B. Yang, H. Mehta, T. Duan, D. Ding, A. Bagul, R.L. Ball, C. Langlotz, K. Shpanskaya, M.P. Lungren, A.Y. Ng, CheXNet: Radiologist-level pneumonia detection on chest X-rays with deep learning, arXiv:1711.05225, 2017.

- [17] Making connections: using networks to stratify human tumors, Benjamin J Raphael, *Nature Methods* 10(11), 1077-1078, 2013.
- [18] S. Saeb, L. Lonini, A. Jayaraman, D.C. Mohr, K. P. Kording, The need to approximate the use-case in clinical machine learning, *GigaScience* 6, 1-9, 2017.
- [19] A. Simón, Métodos Bayesianos para comparar el funcionamiento de algoritmos sobre un conjunto de datos biomédicos, Trabajo de fin de Grado, Universidad Complutense de Madrid - Universidad de Granada, 2020
- [20] J. Soul, S.L. Dunn, S. Anand, F. Serracino-Inglott, J.M. Schwartz, R.P. Boot-Handford, T.E. Hardingham, Stratification of knee osteoarthritis: two major patient subgroups identified by genome-wide expression analysis of articular cartilage, *Annals of the Rheumatic Diseases* 0:1-8, 2017
- [21] S. Valladares-Rodriguez, R. Pérez-Rodriguez, J.M. Fernandez-Iglesias, L.E. Anido-Rifón, D. Facal, C. Rivas-Costa, Learning to detect cognitive impairment through digital games and machine learning techniques, *Methods of Information in Medicine* 57, 197-207, 2018
- [22] W. Vogt, D. Nagel, Cluster analysis in diagnosis, *Clinical Chemistry* 38(2), 182-198, 1992.
- [23] J.H. Ward, Hierarchical grouping to optimize an objective function, *Journal of the American Statistical Association* 58(301), 236-244, 1963.
- [24] Z. He, J. Zhang, X. Yuan, Z. Liu, B. Liu, S. Tuo, Y. Liu, Network based stratification of major cancers by integrating somatic mutation and gene expression data, *PLOS One* 12(5), e0177662, 2017.
- [25] E. Wu, L.M. Hadjiiski, R.K. Samala, H.P. Chan, K.H. Cha, C. Richter, R.H. Cohan, E.M. Caoili, C. Paramagul, A. Alva, A.Z. Weizer, Deep learning approach for assessment of bladder cancer treatment response, *Tomography* 5(1), 201-208, 2019.